Rare Metal Materials and Engineering
Volume 54, Issue 10, October 2025
Available online at www.rmme.ac.cn

Science Press

Cite this article as: Zhou Dapeng, Liu Zhongshu, Huang Jiawen, et al. Interfacial and Mechanical Properties of Cu/Al Composite Plates Manufactured by Rolling and Underwater Explosive Welding[J]. Rare Metal Materials and Engineering, 2025, 54(10): 2461-2469. DOI: https://doi.org/10.12442/j.issn.1002-185X.20240745.

ARTICLE

Interfacial and Mechanical Properties of Cu/Al Composite Plates Manufactured by Rolling and Underwater Explosive Welding

Zhou Dapeng[1,2], Liu Zhongshu[3,4], Huang Jiawen[3,4], Chen Jinhua[1,2], Chen Xiang[3,4], Zhou Xiaohong[1,2]

[1] China Coal Technology Engineering Group Huaibei Blasting Technology Research Institute Co., Ltd, Huaibei 235099, China; [2] Anhui Key Laboratory of Explosive Energy Utilization and Control, Huaibei 235099, China; [3] State Key Laboratory of Precision Blasting, Jianghan University, Wuhan 430056, China; [4] Hubei Key Laboratory of Blasting Engineering, Jianghan University, Wuhan 430056, China

Abstract: Cu/Al composite plates were fabricated using rolling and underwater explosive welding techniques, separately, to compare their interfacial microstructures and mechanical performance. Interface morphology, grain orientation, grain boundary characteristics, and phase distribution were analyzed through optical microscope, scanning electron microscope, and electron backscattered diffractometer. Mechanical properties were assessed using tensile shear tests, 90° bending tests, and hardness measurements. Vickers hardness and nanoindentation test results further provided information on the hardness distributions. Results indicate that the diffusion layer in rolled Cu/Al composites is relatively fragile, while that produced by underwater explosive welding features a diffusion layer of approximately 18 μm in thickness, which is metallurgically bonded through atomic diffusion. The tensile shear strength of these composites ranges from 64.45 MPa to 70.84 MPa, and in the 90° three-point bending test, the underwater-explosive-welded samples exhibit superior flexural performance. This study elucidates the effects of different manufacturing methods on the interfacial properties and mechanical performance of Cu/Al composites, offering essential insights for the selection of manufacturing methods and applications.

Key words: underwater explosive welding; Cu/Al composites; rolling; EBSD; nanoindentation

1 Introduction

With the continuous development of manufacturing technology, Cu/Al composites have received widespread attention due to their lightweight nature, electrical conductivity, thermal conductivity, and corrosion resistance. They have a wide range of applications, particularly in the automobile[1–3], aerospace[4], and marine[5–6] fields. The density of copper is three times larger than that of aluminum, and the melted temperature of aluminum is lower than that of copper by approximately 60%. Therefore, using Cu/Al composites instead of pure copper can significantly reduce the total cost and mass while improving practicality. However, reliable Cu/Al bonding is hard to achieve due to the differences in physical properties of Cu and Al, such as density, melting temperature, and thermal expansion coefficient, which can result in stress and structural inconsistencies at the interface. Effective bonding requires techniques to ameliorate these disparities, therefore enhancing joint quality and durability. Currently, most Cu/Al composites are fabricated using stirring friction[7], rolling, electropulsing[8–9], laser welding[10], and explosive welding[11–14]. These diverse production methods results in diverse interface distributions. Payak et al[15] investigated the stirring friction parameters and the defect evolution of Cu/Al composites, emphasizing the role of interlayers in stirring friction-prepared Cu/Al composites.

Received date: December 18, 2024
Foundation item: Anhui Province Key Research and Development Plan (2022a05020021); China Coal Science and Industry Group Chongqing Research Institute Independent Research and Development Project (2023YBXM58)
Corresponding author: Huang Jiawen, Candidate for Master, State Key Laboratory of Precision Blasting, Jianghan University, Wuhan 430056, P. R. China, E-mail: huangjiawen9944@163.com

Barekatain et al[16] used a typical dynamic shoulder welding technique to fuse AA1050 and pure Cu, and discovered that the material was significantly mixed in the stirring zone with most joints containing both Al and Cu, and voids and cracks can also be observed. Wang et al[17] determined that the grain size and thickness of the diffusion layer are the primary factors influencing the mechanical characteristics of Al/Cu laminated composites. Chang et al[18] performed numerical simulations of as-rolled Cu/Al composites and discovered that the interfacial layer formed in four stages: copper-aluminum surface contact, contact surface activation, mutual diffusion of copper-aluminum atoms, and reaction diffusion. Sas-Boca et al[19] attempted to analyze the bonding of an Al-Cu bimetallic composite layer via hot rolling, but the bonding was inadequate, and the presence of some oxides inhibited bonding, resulting in fissures. Wei et al[20] used explosion welding, cold pressure welding, and solid-liquid casting to create Cu/Al composites and determined that explosive welding is the most advantageous approach. Jiang et al[21] investigated the influence of standoff on the thickness of a localized melted layer in explosively welded Cu/Al.

Rolling over the interface at the solid solution and mechanical occlusion in the thickness direction produces high compressive stress, bonding the metal materials. The main problem of rolling lies in the incomplete metallurgy due to the insufficient diffusion layer. Explosive welding involves the use of explosives to cause two or more layers of the same or dissimilar metals to collide obliquely at the interface, resulting in localized high temperature, high pressure, and substantial plastic deformation[22–24]. The thickness control of melted layer in Cu/Al explosive composites is crucial. Moreover, for thin metal plates[25], it is essential to avoid excessive melting of the interface, parent material breakoff, and other impacts on the quality of the combination. Underwater explosive welding[26] is advantageous because the explosive welding composite device is placed underwater, and water is used to replace air as the propagation medium of the blast energy. This method reduces contact with oxygen and allows the completion of the composite metal plate, which cannot be achieved in air atmosphere. Underwater explosive welding also has advantages in composite thin materials, brittle hard materials, and difficult-to-process materials[27–30].

In this research, Cu/Al composite samples were prepared by rolling and underwater explosive welding, separately. The interfacial microstructure and mechanical properties were analyzed. The morphological properties of the interface, grain orientation, grain boundary features, and phase distribution of the materials were also investigated using optical microscope (OM), scanning electron microscope (SEM), and electron backscattered diffractometer (EBSD). Tensile shear property, 90° bending property, and hardness were obtained to evaluate the mechanical properties, and the Vickers hardness and nanoindentation tests were conducted to analyze the hardness characteristics. This research provided guidance for investigation of the preparation process, interfacial characteristics, and mechanical properties of Cu/Al composites, serving as a reference for optimizing the preparation process and enhancing material qualities.

2 Experiment

This study used two composite methods: rolling and underwater explosive welding. The materials used for rolling and underwater explosive welding were identical with specific parameters, as listed in Table 1. Notably, the surface density of T2 copper is 8.92 $g \cdot cm^{-3}$, while the density of A1060 aluminum is 2.71 $g \cdot cm^{-3}$, indicating a significant difference in their physical properties. The rolled Cu/Al composite plates are commercially available transition plates from LUOYANG COPPER (GROUP) Co., Ltd. A schematic diagram of the underwater explosive welding device for the preparation of Cu/Al composite plates is presented in Fig. 1. To promote effective energy transfer in the water tank, an explosive layer with density of 1.2 $g \cdot cm^{-3}$, explosion velocity of 3500 $m \cdot s^{-1}$, and thickness of 15 mm was fixed beneath the supporting bracket with a distance of 15 mm from the flyer plate. The standoff distance between the flyer plate and the base plate was 0.2 mm. Before welding, the contact surfaces of the Cu and Al plates were prepared through sanding and polishing to improve surface finish and flatness, enhancing contact performance and welding quality.

Microstructure and mechanical property examination of experiment samples involved an in-depth investigation and analysis of the microstructure and properties of the Cu/Al composites. The samples were cut by wire-cutting machine and then processed with resin. The two-dimensional morphology of the samples was examined using OM (ZEISS Axiolab5) and SEM (ZEISS Sigma 300). Energy dispersive spectrometer (EDS) was used for element distribution analysis. EBSD (QUANTA FEG 450 edax) with orientation imaging microscopy analysis software was used to study the grain orientation, grain boundary characteristics, and phase distribution of the samples with a step size of 0.3 μm. The mechanical property tests were also conducted, including tensile shear test, 90° three-point bending test, and hardness test.

3 Results and Discussion

3.1 OM and SEM results

Rolling process was aided by solid solution and mechanical occlusion at the interface, resulting in a relatively thin diffusion layer. Fig. 2 shows OM images of rolled and

Table 1 Material and process parameters

Sample	Material	Process	Medium
1	T2 copper (0.5 mm)+A1060 (4.5 mm)	Rolling	Air
2	T2 copper (2 mm)+A1060 (8 mm)	Underwater explosive welding	Water

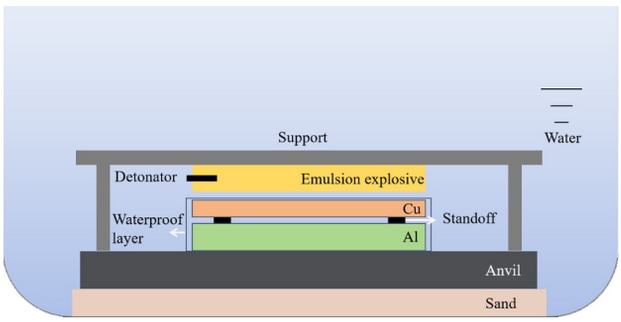

Fig.1 Schematic diagram of underwater explosive welding device

underwater-explosive-welded samples. The presence of the diffusion layer in rolled sample is nearly imperceptible, and the interface is smooth and flat. The oblique collision causes a microwave-like shape of the bonding interface of underwater-explosive-welded samples, which enhances the contact area of Cu and Al and improves the mechanical locking strength of the interface. The impact of the flyer plate on the base plate converts the kinetic energy into thermal energy, resulting in a strong plastic flow of metal and a localized melted layer with thickness of 30 μm.

Fig. 3a–3b and 3d–3e show SEM images at backscattered electron (BSE) mode of the diffusion layer in the rolled and underwater-explosive-welded samples. Fig. 3g shows that the Cu diffusion distance is approximately 1 μm, and the Al diffusion distance is approximately 2 μm, indicating a significant diffusion of Al compared with that of Cu. Vertical cracks perpendicular to the direction of explosive welding can be detected in the melted layer of the underwater-explosive-welded samples, which are caused by thermal strains generated at the interface during rapid solidification at high temperatures[31]. Normally, cracks exist in the melted layer of underwater-explosive-welded samples[32–33], and they tend to form in the thicker part of the melted layer without propagation into the base material. According to EDS analysis results of Fig.3g–3h, the melted layer primarily consists of Al with Al components diffusing into the Cu side. Fig. 3h indicates that Cu diffusion distance is approximately 18 μm and Al diffusion distance is approximately 16 μm. The higher diffusion of Al within the melted layer suggests a significant diffusion capacity of Al. Ref. [34] revealed the temperature dependence of interfacial diffusion between the Al and Cu. The interface temperature in the explosive welding method could exceed 1500 K[35]. The presence of a certain diffusion layer can effectively enhance the bond strength of the interface[36–37]. The diffusion capacity of Al is greater than that of Cu in both the rolled and underwater-explosive-welded samples.

3.2 EBSD analysis results

The kernel average misorientation (KAM) maps are shown in Fig.4c and 4f, and it is found that rolled samples have lower KAM values than the underwater-explosive-welded samples. Normally, the higher the KAM value, the greater the orientation variance within the grains, and the larger the plastic deformation or dislocation density. Although the rolling process can produce persistent compressive stress and plastic deformation, the explosive welding shock wave can produce greater transient compressive stress and local plastic deformation, resulting in more intense compression and plastic deformation for the underwater-explosive-welded samples. In contrast, the lower nuclear mean orientation of the melted layer in underwater-explosive-welded sample (Fig. 4f) indicates that large pressure and plastic deformation occur on both sides of the interface, and the mean orientation is greater on the Al side than on the Cu side, owing to the higher strain caused by the greater compressive stress and plastic deformation on the Al side[38–39]. Enrichment of high-angle grain boundaries (HAGBs) occurs at the interface of underwater-explosive-welded sample (Fig. 4d), but this phenomenon does not occur in the rolled sample. The increase in HAGBs indicates a rise in crystal energy and recrystallization fraction. As shown in Fig. 4e, a large number of fully recrystallized grains are distributed at the interface of underwater-explosive-welded sample, implying a uniform strain distribution. The Cu side of underwater-explosive-welded sample has large recrystallized grains, while the Al side experiences strong plastic deformation, which is about

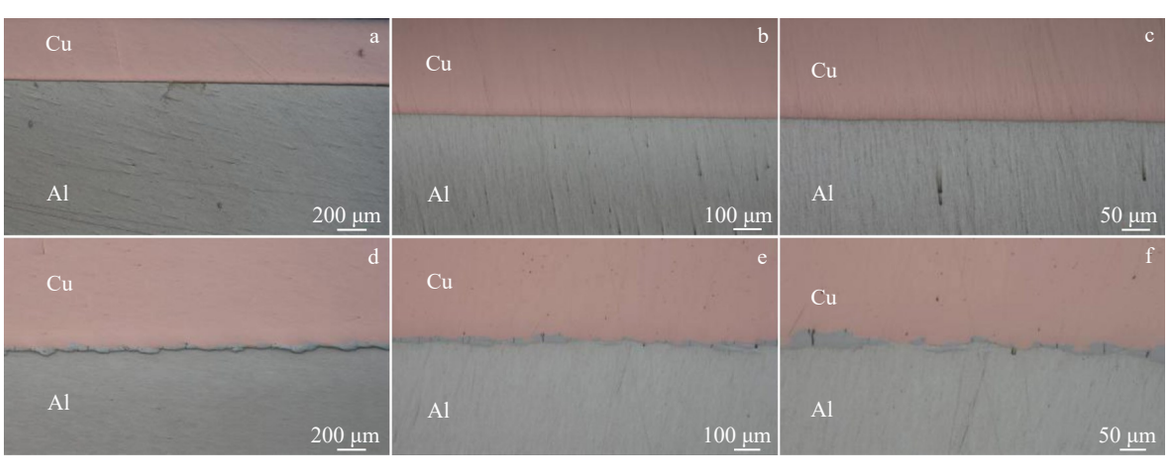

Fig.2 OM images of rolled (a–c) and underwater-explosive-welded (d–f) samples

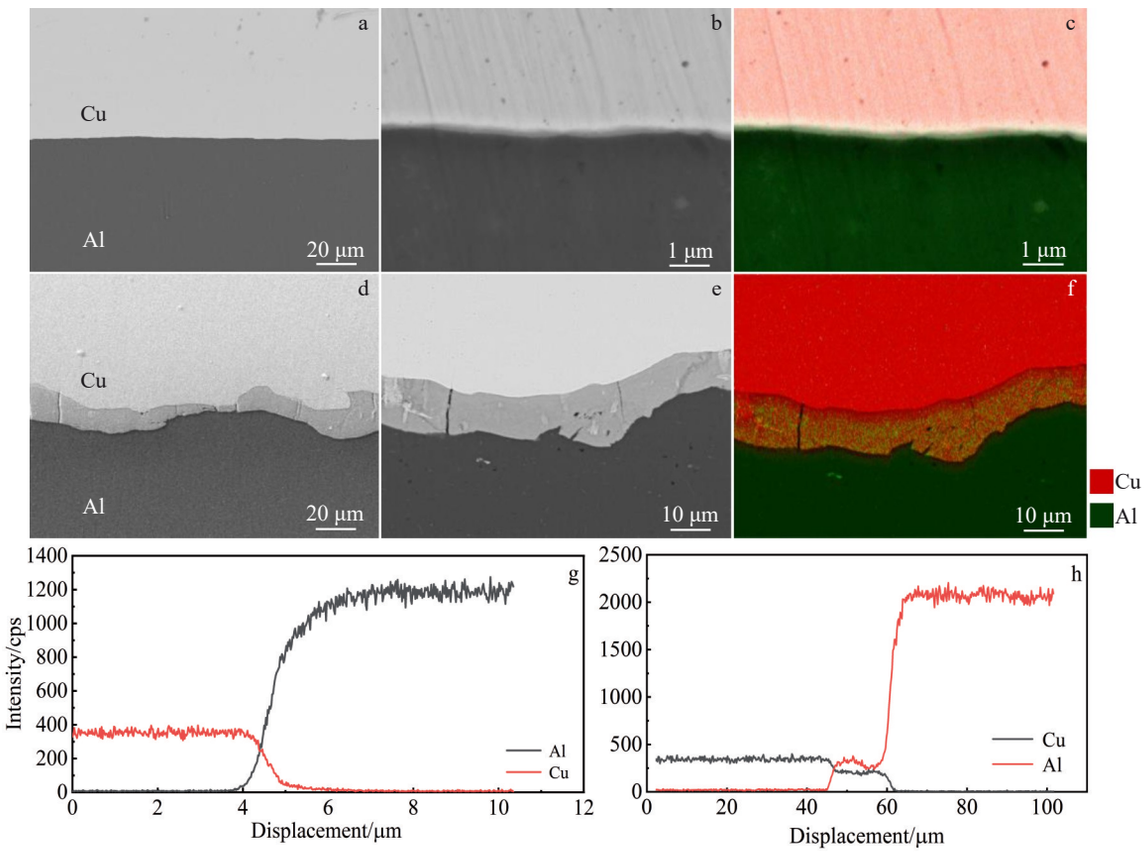

Fig.3 SEM-BSE images (a–b, d–e), EDS element distributions (c, f), and EDS element distribution curves (g–h) of diffusion layer in rolled (a–c, g) and underwater-explosive-welded (d–f, h) samples

10 μm away from the contact surface, resulting in deformed grains. It can be seen that the composites with low stacking fault energy (SFE) are available[40–41]. Cu is prone to dynamic recrystallization and development of equiaxed fine crystals near the interface of underwater-explosive-welded sample due to the high temperature effect which results from the widely extended dislocations. Thus, dislocation climbing is unfavorable. Conversely, Al side with the highest SFE is more vulnerable to deformed grains and dynamic recovery because of the restricted width of the extended dislocations for climbing and cross-slip.

Fig.5a–5b depict the grain distributions between Cu and Cu-Al complexes, namely inverse pole figures (IPFs). Grain refinement occurs along the interface in both rolled and underwater-explosive-welded samples. The grain refinement in the underwater-explosive-welded samples is more obvious. After heating at high temperatures by underwater explosive welding, the diffusion ability of atoms increases, and the grains form fine isometric crystals via re-nucleation. The grain size of the rolled samples is significantly larger than that of the underwater-explosive-welded samples, due to the difference in the base materials and the grain refinement caused by the increased compressive stress and plastic deformation produced by underwater explosive welding. The average grain size of Cu side, Cu-Al compound, and Al side in rolled samples is 5.65, 0.65, and 2.11 μm, respectively; whereas in the underwater-explosive-welded samples, the average grain size of Cu side, Cu-Al compound, and Al side is 0.95, 0.94, and 2.25 μm, respectively. Ultrafine grains (UFGs) are defined as the grain with size less than 1 μm. They can improve mechanical properties of alloys, such as tensile strength[42] and creep behavior[43].

Fig. 6 depicts the texture distributions of Cu/Al composite plates. The interface of Cu/Al composite plates has different textures: deformation textures (S texture {123}<634>, Copper texture {112} <111> , and Brass texture {011} <112>) and recrystallization textures (Goss texture {011}<100> and Cube texture {001}<100>). In the rolled samples, the S and Cube textures are mainly distributed on the Cu side, whereas the Brass texture is predominantly distributed on the Al side. In underwater-explosive-welded samples, the texture irregularity is along the interface, and the recrystallization texture, Goss texture, and Brass texture have the greatest overall dispersion. Compared to the recrystallization distribution map in Fig. 4e, the Goss texture is distributed on the recrystallized grains, whereas the Brass texture is distributed on the deformed grains. Deformation texture generally causes material anisotropy, which is detrimental to mechanical stability[44]. The rolled samples have more deformation textures. As shown in Fig. 7, in the rolled and underwater-explosive-welded samples, the strength of the weave on the Al side of rolled and underwater-explosive-welded samples is 10.90 and 9.84,

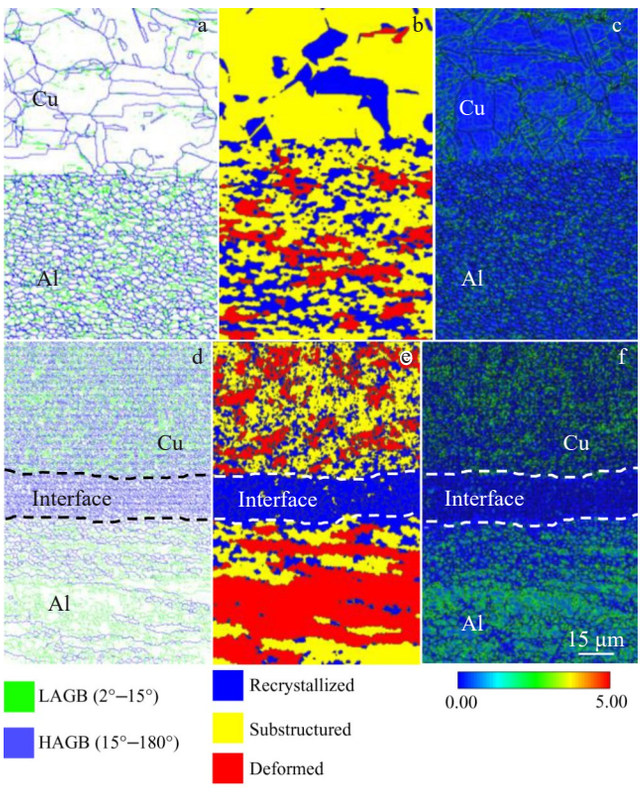

Fig.4 EBSD results of interface of rolled (a – c) and underwater-explosive-welded (d – f) Cu/Al composite plates: (a, d) grain boundary maps; (b, e) recrystallization distribution maps; (c, f) KAM maps

respectively, and that on Cu side of rolled and underwater-explosive-welded samples is 6.51 and 3.26, respectively. This results shows that the strength of the weave on the Al side is higher than that on the Cu side. Dynamic recrystallization hinders the weave transformation[45], weakening the texture, whereas the Cu side is more prone to dynamic recrystallization, resulting in a low-intensity texture.

3.3 Mechanical property analysis

Fig. 8 shows the tensile shear test results of the underwater-explosive-welded samples. Only the underwater-explosive-welded samples were used because the upper layer of the rolled samples was excessively thin (0.5 mm), resulting in difficult sampling. Three samples were used for analysis, and they are denoted as 1-1, 1-2, and 1-3, as shown in Fig. 8b. All samples are fractured at the weld contact with shear strengths ranging from 64.45 MPa to 70.84 MPa. The sample fracture does not exhibit a plateau phase, indicating a brittle fracture. Both Cu and Al have face-centered cubic (fcc) crystal structures, which is generally related to ductile fracture mode. However, after cold working by explosive welding, the dislocation density increases, and the fracture mode is transformed from ductile fracture to brittle fracture. According to Fig. 8d, only Cu can be detected on the Cu side, whereas Al and $AlCu_3$ compound can be detected on the Al side. This result implies that the fracture occurs at the interface between Cu and the melted layer, and the melted layer contains $AlCu_3$ and Al.

Fig. 9 shows the 90° bending test results of rolled and underwater-explosive-welded samples. As shown in Fig. 9a, samples 1-A and 2-A indicate the rolled and underwater-explosive-welded samples with Cu on the outer side, respectively; samples 1-B and 2-B indicate the rolled and underwater-explosive-welded samples with Al on the outer side, respectively. No significant delamination or cracking can be observed in the samples, inferring that all sample can withstand 90° bending from both the Cu and Al sides. However, the measured bending strength of the underwater-explosive-welded samples (277.64 – 343.18 MPa) is significantly larger than that of the rolled samples (234.85 – 257.17 MPa).

Fig. 10 shows the hardness results of rolled and underwater-explosive-welded samples. Vickers hardness was measured with a test weight of 0.2 kg. The hardness of the underwater-explosive-welded samples increases as the test point approaches the contact on the Cu side, and it decreases as the test point approaches the interface on the Al side. Contrarily, the rolled samples show the opposite tendency. Grain refinement also occurs in the rolled samples on the Al side near the interface, as shown in Fig. 5, and the grain refinement contributes significantly to hardness strengthening[46]. Work hardening and grain refinement also contribute to the hardness improvement at the Cu side of the underwater-explosive-welded samples at the contact area. However, strain softening occurs on the Al side during EBSD testing due to high SFE

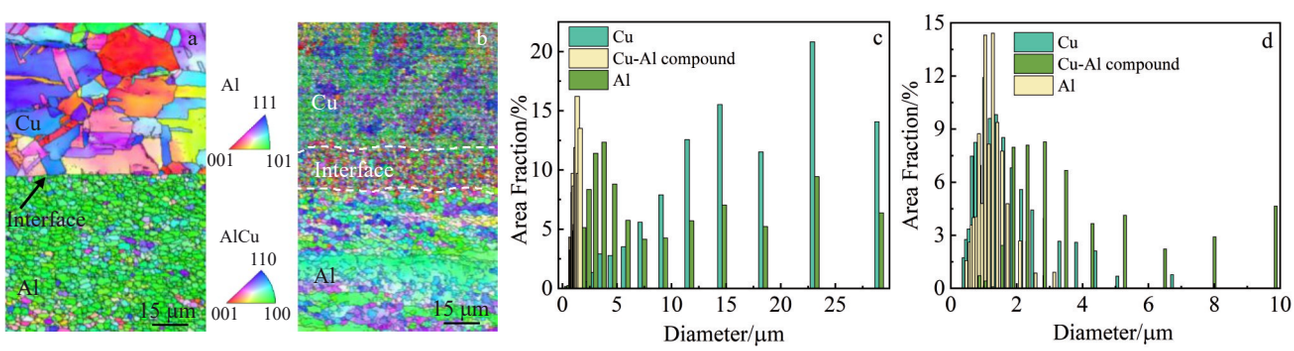

Fig.5 Grain distributions at interface of rolled (a, c) and underwater-explosive-welded (b, d) Cu/Al composite plates: (a–b) IPF maps; (c–d) grain size distributions

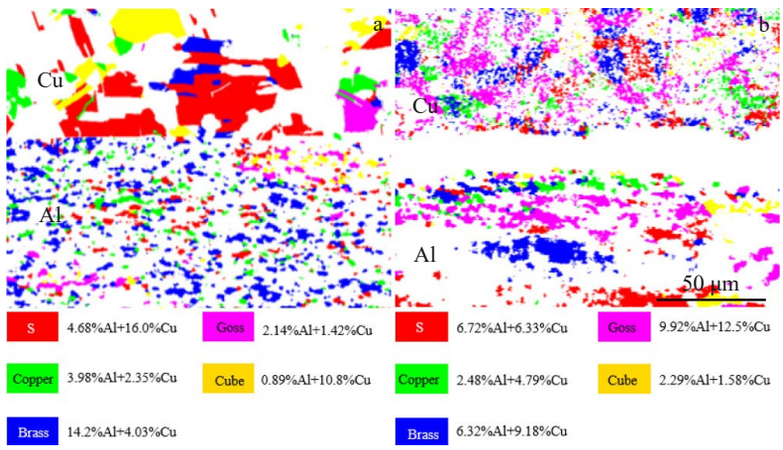

Fig.6 Texture distributions at interface of rolled (a) and underwater-explosive-welded (b) Cu/Al composite plates

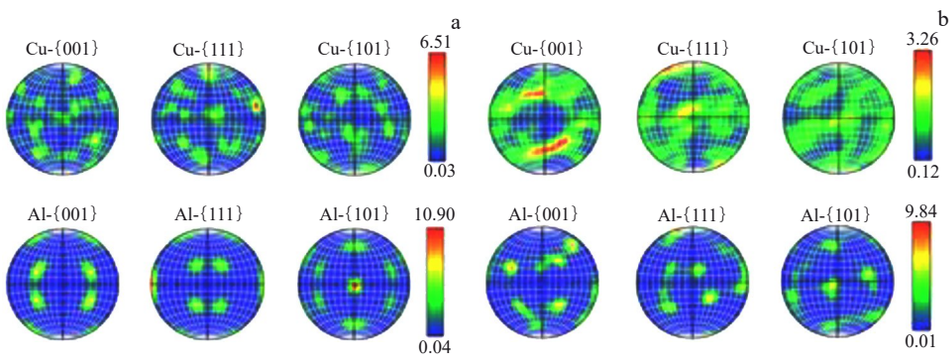

Fig.7 Polar distributions of rolled (a) and underwater-explosive-welded (b) Cu/Al composite plates

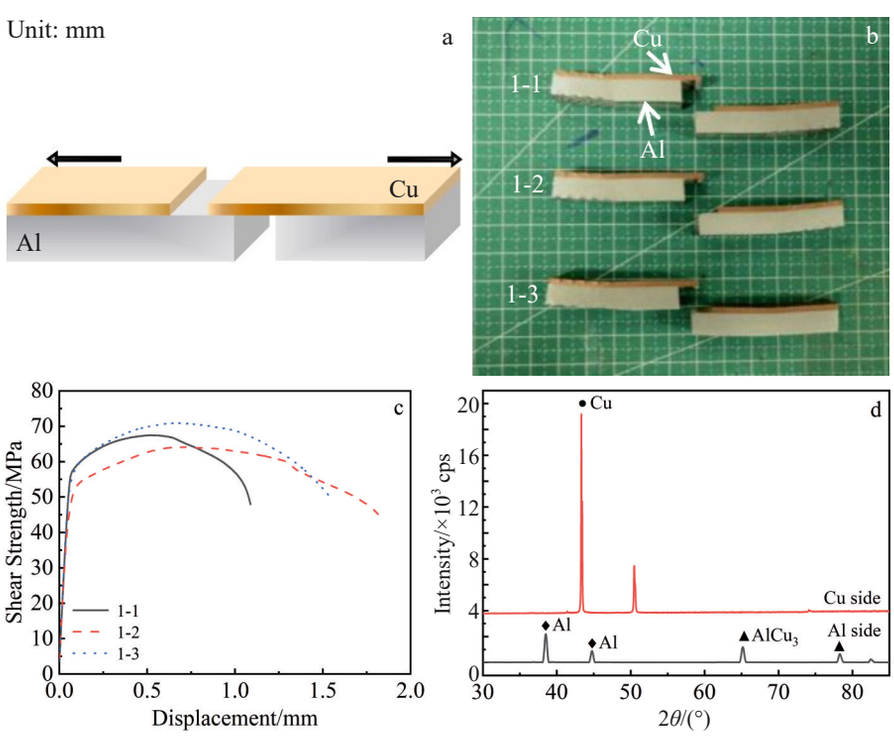

Fig.8 Schematic diagram (a) and appearances (b) of tensile shear samples of underwater-explosive-welded sample; tensile shear curves of different tensile shear samples (c); XRD patterns of fractures on Al and Cu sides (d)

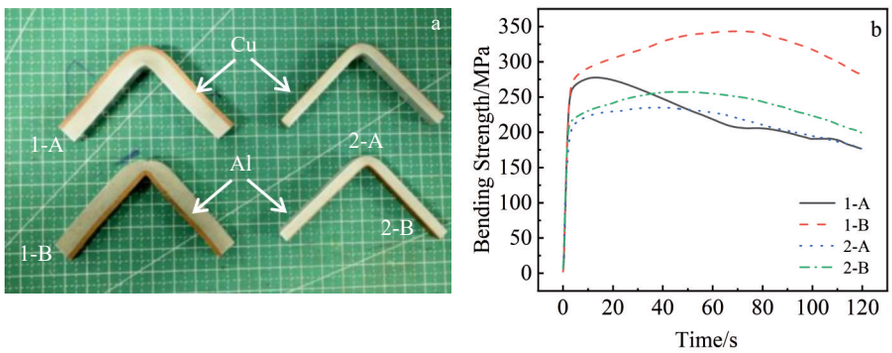

Fig.9 Appearances (a) and 90° bending curves (b) of rolled and underwater-explosive-welded samples

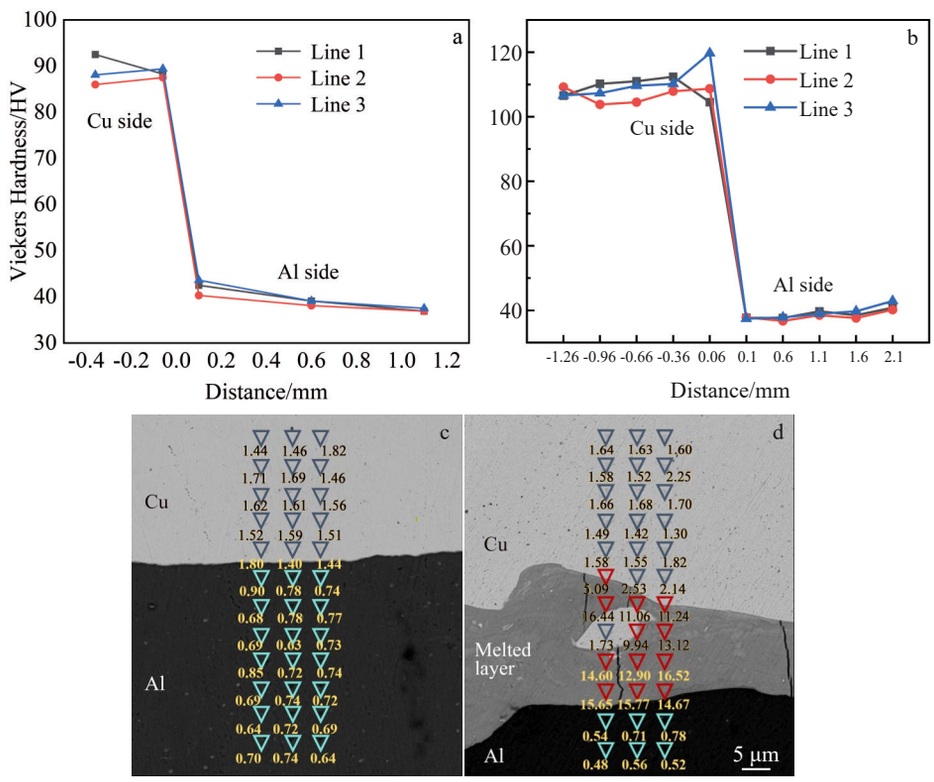

Fig.10 Vickers hardness (a–b) and nanohardness (c–d) results of rolled (a, c) and underwater-explosive-welded (b, d) samples

and dynamic recovery during underwater explosive welding, counteracting work hardening. Therefore, the hardness becomes larger when the area is closer to interface. The nanoindentation experiments were conducted with a test force of 1000 μN. Each point was indented with an interval of 5 μm, and 30 points were used for analysis. Near the interface, both rolled and underwater-explosive-welded samples show a slight increase in hardness, which is consistent with the abovementioned grain refinement phenomenon. The melted layer exhibits much higher hardness than the parent material with a maximum nanohardness of 16.52 GPa, which is attributed to the presence of intermetallic compounds and grain refinement. These metal compounds tend to be hard and brittle. Simultaneously, Cu particles enter the melted layer, while the hardness remains unaffected near the fissures.

4 Conclusions

1) The rolled samples are well bonded at the interface by solid solution and mechanical occlusion. The interface is smooth and flat with a thin diffusion layer of about 2 μm in thickness. The underwater-explosive-welded samples exhibit a microwave-like interface with a diffusion layer of approximately 18 μm in thickness, including $AlCu_3$ compound and Al. The diffusion capacity of Al is stronger than that of Cu in both samples. Both the underwater explosive welding and rolling can cause grain refinement, but the grain refinement phenomenon is more pronounced in underwater-explosive-welded samples, especially in the region near the interface.

2) The high SFE of Al in underwater-explosive-welded samples causes high strain and strong textures due to increased compressive stress and plastic deformation. The

grains are largely distorted on the Al side, whereas on the Cu side, they are recrystallized. In the rolled samples, the dominant texture is the deformation texture S, whereas in the underwater-explosive-welded samples, the recrystallization texture Goss is the dominant texture, which is more beneficial to the stable mechanical properties.

3) The tensile shear strengths of the underwater-explosive-welded samples range from 64.45 MPa to 70.84 MPa, and $AlCu_3$ compound is detected at the fracture. Both the underwater-explosive-welded and rolled samples can withstand the 90° bending, but the measured bending strength of the underwater-explosive-welded samples (277.64–343.18 MPa) is significantly larger than that of the rolled samples (234.85–257.17 MPa).

4) The high hardness in rolled sample results from grain refinement and work hardening. The hardness of the underwater-explosive-welded samples increases as the test point approaches the contact on the Cu side, and it decreases as the test point approaches the interface on the Al side. This is due to the offsetting effects of strain softening and work hardening. The formation of metal compounds in the melted layer significantly enhances nanohardness of both samples.

References

1 Elgallad E M, Samuel F H, Samuel A M *et al*. *Journal of Materials Processing Technology*[J], 2010, 210(13): 1754

2 Kahveci O, Kaya M F. *International Journal of Hydrogen Energy*[J], 2022, 47(24): 12179

3 Li J Q, Zillner J, Balle F. *Materials*[J], 2023, 16(8): 3033

4 Alexopoulos N D, Migklis V, Kourkoulis S K *et al*. *Advanced Materials Research*[J], 2015, 1099: 1

5 Raju P V K, Reddy M I, Harsha N *et al*. *Materials Today: Proceedings*[J], 2018, 5(2): 5845

6 Ziakhor I V, Nakonechnyi A O, Qichen W *et al*. *Electrometallurgy Today/Sovremennaya Elektrometallurgiya*[J], 2023(3): 48

7 Jiang F, Wang W Q, Zhang X G *et al*. *Metals*[J], 2023, 13(12): 1969

8 Zhou Y Y, Jiang F C, Wang Z Q *et al*. *Journal of Materials Processing Technology*[J], 2023, 313: 117884

9 Ran M T, Bian G B, Zhang H W *et al*. *Journal of Manufacturing Processes*[J], 2024, 119: 224

10 Dhara S, Finuf M, Zediker M *et al*. *Journal of Materials Processing Technology*[J], 2023, 317: 117989

11 Tayebi P, Nasirin A R, Akbari H *et al*. *Metals*[J], 2024, 14(2): 214

12 Athar M M H, Tolaminejad B. *Materials & Design*[J], 2015, 86: 516

13 Kaya Y. *Metals*[J], 2018, 8(10): 780

14 Jandaghi M R, Saboori A, Khalaj G *et al*. *Metals*[J], 2020, 10(5): 634

15 Payak V, Paulraj J, Roy B S *et al*. *Journal of Process Mechanical Engineering*[J], 2024, 238(3): 1462

16 Barekatain H, Kazeminezhad M, Kokabi A H. *Journal of Materials Science & Technology*[J], 2014, 30(8): 826

17 Wang Y, Liao Y, Wu R Z *et al*. *Materials Science and Engineering A*[J], 2020, 787: 139494

18 Chang Q H, Gao P K, Zhang J Y *et al*. *Materials*[J], 2022, 15(22): 8139

19 Sas-Boca I M, Iluțiu-Varvara D A, Tintelecan M *et al*. *Materials*[J], 2022, 15(24): 8807

20 Wei Y N, Li H, Sun F *et al*. *Metals*[J], 2019, 9(2): 237

21 Jiang L, Luo N, Liang H *et al*. *The International Journal of Advanced Manufacturing Technology*[J], 2022, 123(9): 3021

22 Blazynski T Z. *Explosive Welding, Forming and Compaction*[M]. New York: Springer Science & Business Media, 2012

23 Rong Kai. *Coal Mine Blasting*[J], 2022, 40(2): 4 (in Chinese)

24 Liu Wu, Xia Zhiyuan, Ma Liubo *et al*. *Coal Mine Blasting*[J], 2020, 38(3): 14 (in Chinese)

25 Hokamoto K, Fujita M, Shimokawa H *et al*. *Journal of Materials Processing Technology*[J], 1999, 85(1–3): 175

26 Zhou Dapeng. *Coal Mine Blasting*[J], 2023, 41(1): 17 (in Chinese)

27 Hokamoto K, Ujimoto Y, Fujita M. *Materials Transactions*[J], 2004, 45(9): 2897

28 Yu Y, Ma H, Zhao K *et al*. *Central European Journal of Energetic Materials*[J], 2017, 14(1): 67678

29 Habib M A, Keno H, Uchida R *et al*. *Journal of Materials Processing Technology*[J], 2015, 217: 310

30 Sun W, Li X J, Yan H H *et al*. *Journal of Materials Engineering and Performance*[J], 2014, 23: 421

31 Kou S. *JOM*[J], 2003, 55: 37

32 Wang K, Kuroda M, Chen X. *Metals*[J], 2022, 12(8): 1354

33 Chen X, Inao D, Tanaka S *et al*. *Journal of Manufacturing Processes*[J], 2020, 58: 1318

34 Li C, Li D X, Tao X M *et al*. *Modelling and Simulation in Materials Science and Engineering*[J], 2014, 22(6): 065013

35 Huang J W, Liang G F, Luo N *et al*. *Journal of Materials Research and Technology*[J], 2023, 27: 2508

36 Bataev I A, Tanaka S, Zhou Q *et al*. *Materials & Design*[J], 2019, 169: 107649

37 Yu Q, Liu X, Sun Y. *Science China Materials*[J]. 2015, 58(7): 574

38 Chen D G, Zhang H M, Zhao D D *et al*. *Materials Letters*[J], 2022, 322: 132491

39 Li X L, Zhang L Q, Su Y *et al*. *Journal of Manufacturing Processe*[J], 2024, 126: 74

40 Bian X Q, Wang A Q, Xie J P *et al*. *Nanotechnology*[J], 2023, 34(44): 445702

41 Wang C, Ma X G, Ma L *et al*. *Materials Characterization*[J], 2023, 205: 113315

42 Martynenko N, Rybalchenko O, Bodyakova A *et al*. *Materials*[J], 2022, 16(1): 105

43 Yang Xirong, Zhu Zhen, Liu Xiaoyan *et al*. *Rare Metal Materials and Engineering*[J], 2019, 48(3): 815 (in Chinese)

44 Han Shunchang. *Phase Transformation and Fractography of the Interface of Explosive Welding*[M]. Beijing: National Defense

Industry Press, 2011: 2 (in Chinese)

45 Aghamohammadi H, Hosseinipour S J, Rabiee S M *et al*. *Materials Chemistry and Physics*[J], 2021, 273: 125130

46 Saikrishna N, Reddy G P K, Munirathinam B *et al*. *Journal of Magnesium and Alloys*[J], 2018, 6(1): 83

轧制和水下爆炸焊接制造的铜/铝复合板的界面和力学性能

周大鹏[1,2]，刘中枢[3,4]，黄佳雯[3,4]，陈金华[1,2]，陈　翔[3,4]，周晓红[1,2]

(1. 中煤科工集团淮北爆破技术研究院有限公司，安徽 淮北 235099)

(2. 爆炸能量利用与控制安徽省重点实验室，安徽 淮北 235099)

(3. 江汉大学 精细爆破全国重点实验室，湖北 武汉 430056)

(4. 江汉大学 爆破工程湖北省重点实验室，湖北 武汉 430056)

摘　要：采用轧制和水下爆炸焊接技术制造了铜/铝复合板，比较了它们的界面微观结构和机械性能。通过光学显微镜、扫描电子显微镜和电子背向衍射技术分析了界面形态、晶粒取向、晶界特征和相分布。通过拉伸剪切试验、90°弯曲试验和硬度测量评估了力学性能，其中维氏硬度和纳米压痕试验进一步揭示了硬度分布。结果表明，轧制的铜/铝复合材料中的扩散层相对较弱，而通过水下爆炸焊接产生的复合材料则具有约18 μm厚的通过原子扩散形成冶金结合的扩散层。这些复合材料的抗拉伸剪切强度介于64.45至70.84 MPa之间，水下爆炸焊接样品在90°三点弯曲试验中表现出更优越的弯曲性能。本研究阐明了不同制造方法对铜/铝复合材料界面性能和力学性能的影响，为选择制造方法和应用提供了重要启示。

关键词：水下爆炸焊接；铜/铝复合材料；轧制；EBSD；纳米压痕

作者简介：周大鹏，男，1977年生，博士，中煤科工集团淮北爆破技术研究院有限公司，安徽 淮北 235099，E-mail：hbzhoudapeng@126.com